Frontiers in

CONDENSED MATTER PHYSICS RESEARCH

Contributors

Epiphane Codjovi
Cristian Enachescu
V. V. Fedorov
Joaquim Fort
Dentcho A. Genov
Debnarayan Jana
Jorge Linares
Andrey K. Sarychev
Vladimir M. Shalaev
Alexandru Stancu
Radu Tanasa
François Varret
V. V. Voronin
Marco Zoli

John V. Chang
Editor

NOVA

LIBRARY OF CONGRESS CATALOGING-IN-PUBLICATION DATA
Frontiers in condensed matter physics research / John V. Chang, (editor).
p. cm.
Includes index.
ISBN 1-59454-829-3
1. Condensed matter--Research. I. Chang, John V.
QC173.456.F76 2005
530.4'1072--dc22 2005030351

Published by Nova Science Publishers, Inc. ✣ New York

CONTENTS

PREFACE

Condensed matter is one of the most active fields of physics, with a stream of discoveries in areas from superfluidity and magnetism to the optical, electronic and mechanical properties of materials such as semiconductors, polymers and carbon nanotubes. It includes the study of well-characterized solid surfaces, interfaces and nanostructures as well as studies of molecular liquids (molten salts, ionic solutions, liquid metals and semiconductors) and soft matter systems (colloidal suspensions, polymers, surfactants, foams, liquid crystals, membranes, biomolecules etc) including glasses and biological aspects of soft matter. This new book presents state-of –art research in this exciting field.

The surface plasmons (SPs) eigenproblem which arises in inhomogeneous metal-dielectric films is studied at resonance conditions in Chapter 1. The authors show that short-range correlations present in the governing Kirchhoff Hamiltonian (KH) result in delocalization of the eigenstates at the center of the spectrum. The delocalization is manifested as a power law/logarithmic singularity for the density of states and SPs localization lengths. Based on the SPs eigenproblem, analytical relationships are derived for the elecromagnetic response of the semicontinuous film in resonance and off-resonance regimes. Experimental studies of linear and non-linear optical processes in correlation to the SPs localization problem are proposed.

It is shown in chapter 2 that recently strong electric fields (up to 10^9 V/cm) have been discovered, which affect the neutrons moving in noncentrosymmetric crystals. Such fields allow for new polarization phenomena in the neutron diffraction and in the optics and provide, for instance, a new method of a search for the neutron electric dipole moment (EDM). A strong interplanar electric field of the crystal and a sufficiently long time for the neutron passage through the crystal for Bragg angle close to $\frac{\pi}{2}$ in the case of Laue diffraction make it possible to reach the sensitivity achieved with the magnetic resonance method using ultra cold neutrons (UCN method).

A series of experiments to study the dynamical diffraction of polarized neutrons in thick (1-10 cm) quartz crystals, using the forward diffraction beam and Bragg angles close to 90°, was carried out in a few last years. Also a new neutron optics phenomena were investigated.

The following effects was first observed:

- the effect of an essential time delay of a diffracting neutron inside the crystal for Bragg angles close to $\frac{\pi}{2}$
- the phenomenon of depolarization of a neutron beam in Laue diffraction by noncentrosymmetric α-quartz crystal;
- the effect of a neutron-optic spin rotation for neutrons passing through a noncentrosymmetric crystal with the energies and directions far from the Bragg ones.

The feasibility of an experiment to search for the neutron electric dipole moment (EDM) by Laue diffraction in crystals without a center of symmetry was tested. It was shown that the sensitivity can reach $(3 - 6) \cdot 10^{-25}$ $e \cdot$ cm per day for the available quartz crystal and cold neutron beam flux.

Chapter 3 discusses the Holstein and the Su-Schrieffer-Heeger (SSH) Hamiltonian, which present a fundamental difference with respect to the nature of the *e-ph* coupling. Mapping the real space interactions onto the time scale the authors show that the Holstein *e-ph* interactions are *local* in time while, in the SSH model, the electronic hopping induces a time dependent lattice displacement thus leading to a *non local e-ph* coupling. As a consequence the source current peculiar of the SSH model depends both on time and on the electron path coordinates. The authors apply the path integral method to analyse the perturbing effects of the source currents on the phonon subsystems by expanding the phonon partition function in cumulant series: in the low temperature limit, the constraint imposed by the third law of thermodynamics permits to determine the cutoff in the anharmonic expansions and to point out the different behaviors of the model Hamiltonians. Looking at the equilibrium thermodynamic properties they find striking differences between the Holstein and the SSH model. The Holstein phonon heat capacity does not show any trace of anharmonicity induced by the *e-ph* coupling while the SSH phonon heat capacity exhibits a peak whose location along the T axis strongly depends on the strength of the coupling α. By increasing α at a fixed T, the phonon partition function becomes larger. As a result the point of *most rapid decrease* in the SSH phonon free energy versus temperature shifts downwards and the associated heat capacity peak is found at lower T. At high temperatures the free energy decreases regularly and the anharmonic effects on the heat capacity are reduced.

Finally, the authors compute the general path integral in the SSH model for an electron path moving in a bath of anharmonic oscillators and derive the total heat capacity of the system versus temperature. The contribution of the anharmonic phonons with respect to the purely electronic and *e-ph* terms is discussed. The anharmonic effects are relevant in the intermediate temperature range whereas the peak is smeared by the electronic hopping term (on the low temperature side) and by the source action heat capacity at high temperatures.

A peculiar upturn in the SSH total heat capacity over temperature ratio is found at low T thus pointing to a glassy like behavior for the polymeric chain to which the SSH model applies.

Spin crossover solids are molecular compounds, switchable between two states with different optical and magnetic properties: the low spin (LS) state and the high spin (HS) state. Due to elastic interactions, some of these compounds (the spin-transition solids) show a complex nonlinear behavior including temperature, pressure, and light-induced thermal

hysteresis (TH, PH and LITH) that makes them strong candidates for optical display and ultra-high density data storage. Studying hysteretic behavior of spin transition compounds the authors have applied for the first time in a systematic manner the Preisach-type models, and they have observed that the experimental data are compatible with some statistical distributions of the physical properties of the system constituents. For the materials correctly described by the Classical Preisach Model (CPM systems) the distributions could be directly linked with some physical properties of the material. Recently, the First Order Reversal Curves (FORC) experimental technique of Preisach distribution calculation was applied as a general identification method for non-CPM systems. The authors have applied the FORC diagram method for TH and have shown that the diagram can be interpreted in terms of distributions of physical parameters such as the energy gap between the LS and HS states and a mean field interaction parameter. In chapter 4, they shall present the general FORC diagram method and how the method can be applied for other hysteresis types, like the TH. The FORC method applied on pure and diluted spin transition materials $[Fe_xZn_{1-x}(btr)_2(NCS)_2]\cdot H_2O$ has suggested distributions of internal stresses and domain size, increasing with dilution $(1-x)$. In addition, they present experimental FORC data for LITH, i.e. for the thermal hysteresis of the system submitted to a constant photo-excitation. The authors describe the models adapted to both TH and LITH, so as to simulate the FORC curves of the LITH, and we discuss the origin of the similarities and differences between experimental data and simulations, in terms of the physical constraints of the LITH experiments. In the paper they also discuss the main error sources associated with the experimental FORC diagram method and the problem of the diagram accuracy.

Mott first pointed out the importance of electron's Variable Range Hopping (VRH) between the localized states in discussing the conduction process of disordered insulators at low temperature. Chapter 5 uses VRH Model to compute the Mott conductivity of an interacting amorphous system in an arbitrary dimension d. The characteristic feature of this interacting system is the existence of a soft gap at the Fermi energy. The authors found that both at low as well as at high electric field, the values of the exponents characterizing the behavior of conductivity in this interacting system are always higher than that of non-interacting ones in all spatial dimensions. They also obtain the bound (lower as well as upper) of the values of exponents in contrast to non-interacting case. Finally, this approach allows us to construct a simple form for A.C. conductivity as a function of frequency. They also indicate a general form of the conductivity as a function of electric field and temperature for this system in any arbitrary dimension d. The scaling approach adopted here to study the Mott conductivity gives one the generalized forms of the exponents from which all the previously known results can be obtained. All these may shed light to interpret the experimental conductivity results of amorphous systems at low temperature.

In: Frontiers in Condensed Matter Physics Research
Editor: John V. Chang, pp. 1-11
ISBN 1-59454-829-3

Chapter 1

SURFACE PLASMONS EXCITATION IN SEMICONTINUOUS METAL FILMS

***Dentcho A. Genov*[1], *Vladimir M. Shalaev*[1] *and Andrey K. Sarychev*[2]**
[1]School of Electrical and Computer Engineering, Purdue University,
West Lafayette, Indiana 47907, USA
[2]Ethertronics Inc., San Diego, CA 92121, USA

Abstract

The surface plasmons (SPs) eigenproblem which arises in inhomogeneous metal-dielectric films is studied at resonance conditions. We show that short-range correlations present in the governing Kirchhoff Hamiltonian (KH) result in delocalization of the eigenstates at the center of the spectrum. The delocalization is manifested as a power law/logarithmic singularity for the density of states and SPs localization lengths. Based on the SPs eigenproblem, analytical relationships are derived for the elecromagnetic response of the semicontinuous film in resonance and off-resonance regimes. Experimental studies of linear and non-linear optical processes in correlation to the SPs localization problem are proposed.

1 Introduction

The localization of the electron wavefunction, which occurs in inhomogeneous media and was first described by Anderson [1], is one of the most important concepts in the contemporary theory of disordered systems. Development of the scaling theory [2], improved and made possible more intuitive understanding of the phenomena governing the motion of the elementary particles in such media. It is now well established that in 1D and 2D systems described by non-correlated random potential distributions, all electron states are exponentially localized [3, 4]. This is valid for various levels of disorder and in the limit of large (infinite) systems. The localization of the electron wavefunction implies that each electron is bound in a particular region of space, and thus transport through the media is impeded. It is also believed that in the 3D case and for a certain strength of disorder, extended states exist, and accordingly a metal-dielectric transition may take place [5, 6]. Similar to the quantum-mechanical problem, localization is also observed for classical wave-propagation

in disordered media [4]. In both cases, disorder prevents the establishment of extended solutions (Bloch states) due to the absence of translation symmetry.

A remarkable shift in the studies of the Anderson transition problem have occurred in the last decade. Short-range correlations between the elements of the quantum-mechanical Hamiltonians have been found to result in delocalization of the electron wavefunction in the 1D case [7, 8, 9]. It is not clear whether long-range correlations can also lead to delocalization of the eigenmodes and promotion of metal-insulation transition [10, 11]. In the above cited studies, the correlations are enforced separately for diagonal and off-diagonal matrix elements, while mixed cross-correlations between the elements are not considered. Here, we argue that the electromagnetic response of a broad class of physical systems can be described by random Hamiltonians that are characterized by cross-correlated diagonal and off-diagonal elements. Specifically, we study surface plasmons (SPs) eigenproblem that arises when incident light interacts with local inhomogeneities of the metal-dielectric interfaces. In this problem, conservation of the local currents introduces a correlations between the elements of the Hamiltonian and results in a unique localization-delocalization transition for the collective electronic response. The SPs transition is manifested through a continuous band of localization lengths which diverge at the center of the spectra. The nature of the SPs localization determines the peculiarities in the distributions of the local fields in the composite. Localized and delocalized modes are simultaneously excited at the film surface, with the former corresponding to energy accumulation in small spatial areas and strong fluctuations of the local fields, while delocalized modes are responsible for the transport through the system. The SPs localization properties directly influence the linear and nonlinear optical response of the media.

2 Semicontinuous Films and the Problem of Surface Plasmons Excitation

The random metal-dielectric composites (also known as semicontinuous films) are a special type of disordered media in which the quantum-mechanical and classical processes are intertwined in the establishment of local fields and current distributions. Arguably, the most widespread method for manufacturing the random films is by sputtering or depositing nanometer sized metal particles on dielectric surfaces. With deposition and the subsequent increase in metal concentration, fractal clusters form and grow on the surface. When the metal concentration p exceeds some critical value p_c (refereed to as a percolation threshold), a "backbone" cluster which span the entire system is found. Therefore the composite undergoes a geometrical type phase transition where, for $p < p_c$ it behaves as a dielectric, while for $p \geq p_c$ a metal state is established. With the alternation of film morphology a drastic change in the optical response takes place. This is due to increased coupling of the incident electromagnetic radiation with the collective electronic response (surface plasmons) of the system.

Qualitative understanding of the SPs excitation in random composites is possible through a simple phenomenological model. Within the visible and infrared spectral range, the metal conductivity σ_m is a complex number with a positive imaginary part σ_m'', and a small real part σ_m' (representing losses in the metal). Therefore, the metal particles may be

viewed as an inductance L connected in series to a resistance R. The dielectric host, which is the second constituent of the binary metal-dielectric film, is modeled as a capacitance C. Relying on this similarity, the random metal dielectric film may be considered as a network of RLC circuits, where R, L, and C assume random values [12, 13]. The geometrical disorder in such systems leads to a broad range of plasmon resonances (corresponding to equivalent RLC resonances) and strong enhancement of the local electric fields [13, 14].

To investigate the surface plasmons modes that are excited at the film surfaces, we restrict our study to composites of metal particles with sizes much smaller than the wavelength of illumination, $a \ll \lambda$. Under this condition one we neglect retardation effects and seek a solution for the local potential in the quasi-static approximation. The resulting "generalized" current conservation has the form

$$\nabla \cdot [\sigma(\mathbf{r})(-\nabla\varphi(\mathbf{r}) + \mathbf{E}_0)] = 0, \tag{1}$$

where $\sigma(\mathbf{r})$ is the spatially dependent local conductivity, $\varphi(\mathbf{r})$ describes the local potential and $\mathbf{E}_0$ is the external field. In our model we assign to $\sigma(\mathbf{r})$ a metal conductivity σ_m with probability p, or a dielectric conductivity σ_d with probability $1-p$. Discretization of Eq. (1) on a square lattice with size L leads to a system of L^2 linear equations $\hat{\mathbf{H}} \cdot \mathbf{\Phi} = \mathbf{F}$, where the matrix $\hat{\mathbf{H}}$ is the so called Kirchhoff Hamiltonian (KH), while the vectors $\mathbf{\Phi}$ and $\mathbf{F}$ are the local potentials and externally induced currents, respectively. The KH is a sparse random matrix with diagonal elements given by the sum $H_{ii} = \sum_j \sigma_{ij}$ of all bond conductivities σ_{ij}, that connect the i-th site with its nearest neighbors and off-diagonal elements $H_{ij} = -\sigma_{ij}$. Due to the random nature of the bond conductivities σ_{ij} the KH is thus mathematically similar to the Anderson Hamiltonians (AH) that are studied in quantum mechanics [3, 13]. However, unlike the AH, the diagonal and off-diagonal elements of the KH are not independent. The correlations are due to the local current conservation, and we will show that they result in dramatic changes in the nature of the SPs localization as compared to the discrete non-correlated Anderson analogue.

In order to simplify the treatment of the SPs excitation in metal-dielectric films, we first work in the regime of single particle resonance $\varepsilon'_m = -\varepsilon_d$, where the dielectric constants $\varepsilon_s = 4\pi i\sigma_s/\omega_r$ depend on the complex conductivities σ_s (s stands for the metal or the dielectric components) and the resonance frequency ω_r. Next, we normalize Eq. (1) by σ_d and then use a new set of non-dimensional permittivities $\varepsilon^*_d = 1$ and $\varepsilon^*_m = -1 + i\kappa$, where for noble metals and visible light the losses are small $\kappa = \varepsilon''_m/|\varepsilon'_m| \ll 1$. Following the perturbation theory [13], we seek a general solution of Eq. (1) as an expansion over the eigenstates Ψ_n of the SPs eigenproblem

$$\nabla \cdot [\theta(\mathbf{r})\nabla\Psi_n(\mathbf{r})] = \Lambda_n\Psi_n(\mathbf{r}), \tag{2}$$

where the topology function $\theta(\mathbf{r}) = \pm 1$ maps the the real part of the non-dimensional dielectric constant $\varepsilon^*(\mathbf{r})$, and thus corresponds only to the geometrical characteristic of the film. Reduction of Eq. (2) on a square lattice results in a matrix equation $\hat{\mathbf{H}}' \cdot \mathbf{\Psi}_n = \Lambda_n\mathbf{\Psi}_n$, where $\hat{\mathbf{H}}'$ is the real part of the normalized KH and has the same correlation properties. These correlations can also be represented with the covariance matrixes $\hat{\mathbf{G}}^{d-d}$and $\hat{\mathbf{G}}^{d-o}$that describe the statistical dependences between the diagonal $\{d_i\}$ and off-diagonal $\{o_i\}$ elements of the matrix $\hat{\mathbf{H}}'$. Specifically, for the diagonal elements we have $G^{d-d}_{ij} =$

$E[(d_i - \overline{d})(d_j - \overline{d})] = \sigma_o^2(\delta_{i,j\pm1} + \delta_{i,j\pm L} + 4\delta_{ij})$, where E is the expectation value, σ_o is the standard deviation of the off-diagonal elements and δ_{ij} is the Kronecker delta function. The correlations between diagonal and off-diagonal elements are given by $G_{ij}^{d-o} = E[(d_i - \overline{d})(o_j - \overline{o})] = \sigma_o^2(\delta_{i,j-1} + \delta_{ij})$, where we have taken into consideration the first to the right off-diagonal vector, but similar relationships hold for the rest of the off-diagonal vectors. For all cases, at the percolation threshold $p = p_c = 1/2$ we have $\sigma_o = 1$ and $\overline{d} = \overline{o} = 0$.

In the solution of Eq. (2) we impose Neumann-type boundary conditions, thus assuring the conservation of the local currents at the film boundaries. For example, we use $\theta(\mathbf{r})[\mathbf{n} \cdot \nabla\Psi_n(\mathbf{r})]|_{x=0} = \theta(\mathbf{r})[\mathbf{n} \cdot \nabla\Psi_n(\mathbf{r})]|_{x=L}$ at the left and right boundaries. Alternatively, one may apply an electrode type boundary $\Psi_n(\mathbf{r})|_{x=0} = \Psi_n(\mathbf{r})|_{x=L} = const$ or "natural" boundary conditions where $\Psi_n(\mathbf{r})|_{edge} = 0$ for all four sample borders. However, our studies show that for large systems and strong disorder ($p = p_c$), the statistical properties of the SPs eigenproblem are virtually independent on the boundary conditions.

3 Density of States and Surface Plasmons Localization Lengths

We start the analysis of the SPs eigenproblem by examining some specific eigenmodes that are presented in the spectra. For random metal-dielecric films at the percolation threshold, we are able to distinguish two limiting cases. In the first case shown in Fig. 1a, the SPs eigenmodes situated at the edge of the spectral band ($\Lambda \simeq \Lambda_b$) are strongly localized. The localization lengths of those states correspond to the Anderson localization lengths ξ_A of the statistically equivalent non correlated eigenproblem. Examination of the SPs eigenmodes at the band center (see Fig. 1b) shows a completely different picture. Those states are extended and in accordance to our studies (not presented here) they exhibit multifractal properties. In Fig. 1c,d we also present two SPs modes that are manifested in the periodic case. The periodic structure is modeled as a square lattice of metal particles with metal coverage equal to $2/3$. The important feature to be recognized here is the presence of two length scales, one corresponding to the macroscopically extended Bloch states, and the second to local oscillations on the scale of a single particle. We believe the microscopic SPs eigenmode fluctuations are a blueprint of the strong inhomogeneity of the electromagnetic fields that are observed even for perfectly ordered metal-dilectric nanosystems [15].

The statistical properties of the SPs eigenproblem are investigated in terms of the density of states $\rho(\Lambda)$ and localization lengths $\xi(\Lambda)$. Both characteristics are studied for the KH and the corresponding discrete, non-correlated AH. As previously mentioned, for each metal concentration p the diagonal elements of matrix $\hat{\mathbf{H}}'$ (at the resonance, $\varepsilon_d = -\varepsilon_d = 1$) take discrete values with a specific probability. For example, the matrix element H'_{ii} takes values ± 2 with probabilities $4p(1-p)^3$ and $4p^3(1-p)$ respectively. The most probable value for the diagonal matrix elements is zero, and its probability is $6p^2(1-p)^2$. The analytical distributions of the matrix elements can be used to simulate one equivalent (for $p = 1/2$), non-correlated AH and compare the results with those for the KH.

In Fig. 2 we show that both correlated and non-correlated eigenvalue problems have quite similar densities of states for most of the spectra. However, at the band center we observe a singularity in the case of the KH. To better understand this peculiarity, we plot (see the insert in Fig. 2) the region of very small eigenvalues ($\Lambda \ll 1$) on a log-log scale. In the

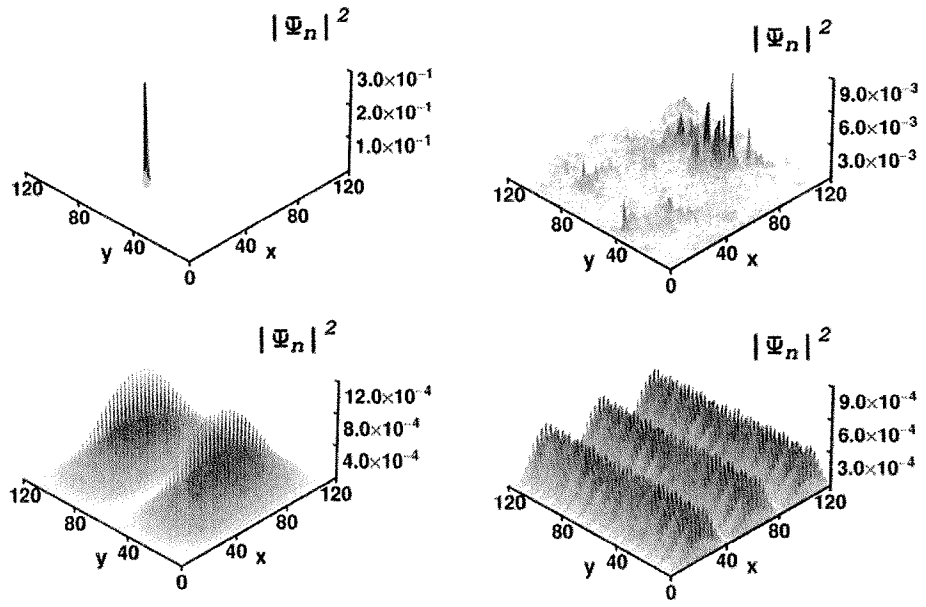

Figure 1: Surface plasmon eigenmodes in random **a**,**b**) and periodic **c**,**d**) metal-dielectric films. The corresponding eigenvalues are: **a**) $\Lambda = -5.6945$ (localized), **b**) $\Lambda = 0.0044$ (delocalized), **c**) $\Lambda = -5.9974$ and **d**) $\Lambda = 0.7033$.

first approximation the density of states seems to diverge as a power law $\rho(\Lambda) \simeq A|\Lambda|^{-\gamma}$, where A is a normalization constant and $\gamma = 0.14 \pm 0.01$ is some exponent. Note that $\rho(\Lambda) \simeq A(1 - \gamma \ln(|\Lambda|)$ also fits the results. These two functions are virtually identical in broad range of the arguments $e^{1/\gamma} \gg \Lambda \gg e^{-1/\gamma}$, and thus for simplicity we use exclusively the power law relationship. In Fig. 2 we also include our result for the non-correlated case, where the density of states is relatively uniform throughout the spectra and does not show any singularity, consistent with our expectations.

The impact of the cross-correlations presented in the KH are also studied in terms of the SPs localization lengths $\xi(\Lambda)$. The localization length for each eigenmode is calculated using the gyration radius

$$\xi^2(\Lambda_n) = \int (\mathbf{r} - \langle \mathbf{r} \rangle)^2 |\Psi_n(\mathbf{r})|^2 d\mathbf{r} \tag{3}$$

where $\langle \mathbf{r} \rangle_n = \int \mathbf{r} |\Psi_n(\mathbf{r})|^2 d\mathbf{r}$ is the "mass center" of the $n - th$ mode and the integration is performed over the film surface. The results for the KH and for the AH are presented in Fig. 3. Similar to what we have observed for the density of states (see Fig. 2), there is a singularity at the band center in the case of the KH which is not present for the AH. The SPs eigenmode localization lengths diverge for $\Lambda \to 0$ as $\xi(\Lambda) \simeq \xi_A |\Lambda_b/\Lambda|^\alpha$, where ξ_A is the Anderson localization length (corresponding to the AH), $\alpha = 0.15 \pm 0.02$ and $|\Lambda_b| \simeq 7$ is the cutoff (band edge) eigenvalue. The size effect is also clearly visible for the extended states with $\xi(\Lambda) \gg L$, where the SPs localization length becomes a constant proportional to the system size L. Delocalization of the eigenstates has also been observed for a different

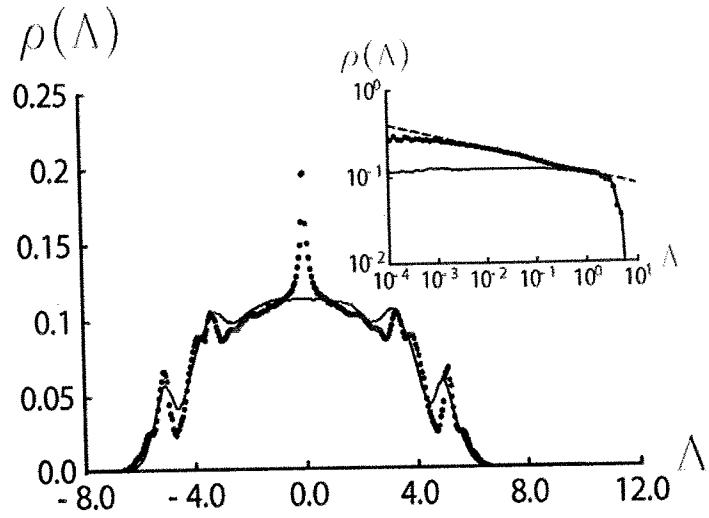

Figure 2: The density of states $\rho(\Lambda)$ for the Kirchhoff Hamiltonian (dots) and for the corresponding Anderson problem (solid line) calculated at the resonance condition $\varepsilon_d^* = -\varepsilon_m^* = 1$ and for critical concentrations ($p = 1/2$). The band-center singularity is shown in the log-log inset where a power law fit (dashed line) with exponent $\gamma = 0.14$ is applied. The data is averaged over 500 different realizations of percolating systems each with size $L = 120$.

plasmon eigenproblem [16]. The authors claim that localized modes cannot be effectively coupled to the external field, and thus only extended (See Fig 1b) modes are luminous. Our results show that all modes are in fact localized, but the localization length itself diverges at the center of the spectra. The delocalized modes investigated in [16] are only a by-product of a finite size effect when $\xi(\Lambda) > L$. In the limit of infinite systems, the density of those eigenstates vanishes as $L^{-1/\gamma}$.

4 High Order Field Moments for Resonance and Off-Resonance Frequencies

The localization of the SPs eigenmodes results in dramatic fluctuations of the local electric fields at the metal-dielectric interfaces. These fluctuations correspond to energy accumulation in nanoscale and are manifested through strong enhancement of a variety of linear and nonlinear optical process. The optical response of the semicontinuous films at the percolation threshold can be very broad in terms of the incident beam frequencies. For example, one can observe anomalous absorption in the near-infrared spectra as well as gigantic enhancement of the second harmonic generation, Raman scattering, Kerr optical nonlinearity,..etc.. In Fig 4 we have shown the enhancement of the local field intensity $I(\mathbf{r}) = |\mathbf{E}(\mathbf{r})/\mathbf{E}_0|^2$ for three particular wavelengths. For all three cases the local field intensities reach values that exceed by more than 10^4 times the applied field intensity. The

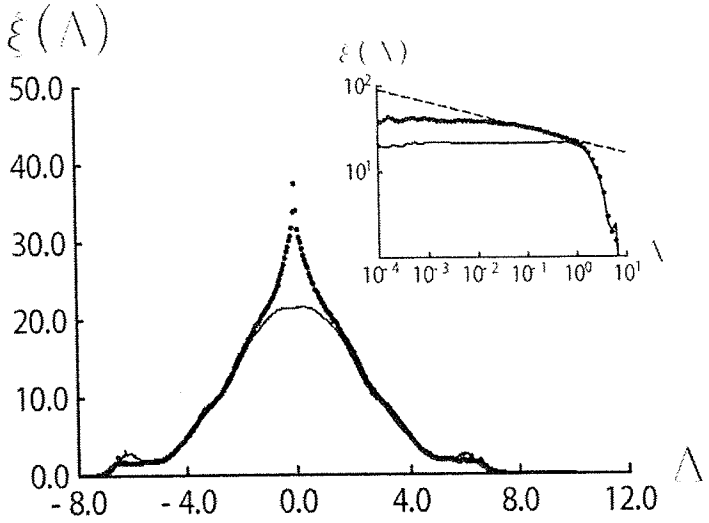

Figure 3: The SPs eigenmode localization lengths $\xi(\Lambda)$ for the correlated KH (dots) and non-correlated AH (solid line). The dashed line in the inset corresponds to a power-law fit. The data is averaged over 20 different realizations of random samples each with size $L = 120$.

amplitudes and distances between the fields peaks are seen to increase with wavelength. These effects are shown below to result directly from the SPs localization-delocalization properties manifested for strongly interactive (at critical metal concentrations) systems.

Relying on the scaling properties of the SPs localization lengths $\xi(\Lambda)$ and the density of states $\rho(\Lambda)$, it is possible to estimate the ensemble averaged high-order moments

$$M_{n,m} = \left\langle \frac{1}{S} \int \frac{|\mathbf{E}(\mathbf{r})|^n [\mathbf{E}(\mathbf{r}) \cdot \mathbf{E}(\mathbf{r})]^{m/2}}{|\mathbf{E}_0|^n [\mathbf{E}_0 \cdot \mathbf{E}_0]^{m/2}} d\mathbf{r} \right\rangle \tag{4}$$

of the local electric fields $\mathbf{E}(\mathbf{r}) = -\nabla\varphi(\mathbf{r})$, where the integration is over the film surface. To accomplish this, we follow the approach developed in [13] and expand the local potential $\varphi(\mathbf{r}) = \int a(\Lambda)\Psi(\Lambda, \mathbf{r})d\Lambda$ over the SPs eigenstates $\Psi(\Lambda, \mathbf{r}) = \Psi_n(\mathbf{r})$. In zero approximation the coefficients $a^{(0)}(\Lambda) = \Pi_{\mathbf{E}_0}(\Lambda)/(\Lambda + i\kappa)$ depend on the projection $\Pi_{\mathbf{E}_0}(\Lambda) = \int \Psi(\Lambda, \mathbf{r})[\mathbf{E}_0 \cdot \nabla\varepsilon(\mathbf{r})]d\mathbf{r}$ of the external field $\mathbf{E}_0$ on the eigenstates. Assuming exponential localization of the SPs eigenmodes with localization length $\xi(\Lambda)$, it is possible to obtain a simple scaling relationship for the high order field moments of the form

$$M_{n,m} \simeq \int_{-\infty}^{\infty} \frac{\rho(\Lambda)[a/\xi(\Lambda)]^{2(n+m-1)}}{(\Lambda^2 + \kappa^2)^{(n+m)/2}} e^{im\phi(\kappa,\Lambda)} d\Lambda \simeq \kappa^{-\varkappa_{n,m}} e^{i\psi_{n,m}(\kappa)} \tag{5}$$

where $\varkappa_{n,m} = (n + m - 1)(1 - 2\gamma) + \gamma$ is a positive scaling exponent ($n + m \geq 1$) and $\phi(\kappa, \Lambda) = \tan^{-1}(\kappa/\Lambda)$ is a phase factor. The general form of the nonlinear phase $\psi_{n,m}(\kappa)$ is a very cumbersome function and is not shown here. In the derivation of Eq. (5) we use

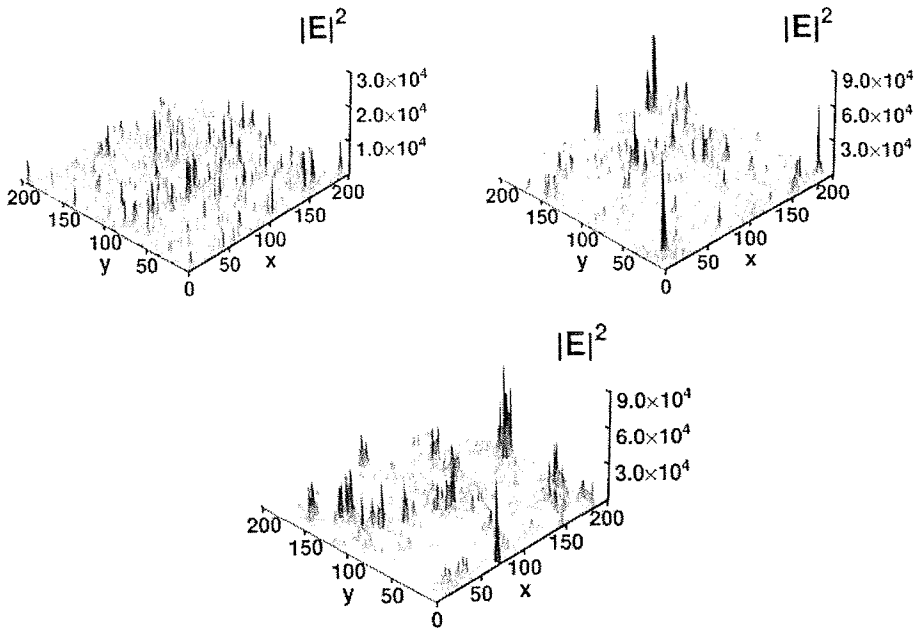

Figure 4: The local field intensities are calculated for percolating ($p = p_c$) silver metal-dielectric film of size $L = 200$. The wavelengths of the incident light are: **a)** $\lambda = 0.5\mu m$, **b)** $\lambda = 1\mu m$ and **c)** $\lambda = 5\mu m$.

$\alpha = \gamma$, which corresponds to our numerical results.

It is also possible to recover the same expression if one considers the local fields as a set of peaks with characteristic size $l_p^* \sim \xi(\kappa)$, magnitude $E_m^* \sim E_0 \kappa^{-1+2\gamma}$, and separation distance between them proportional to $\xi_e^* \sim l_p^* \kappa^{(-1+3\gamma)/2}$. Based on this similarity, the solution presented in Eq. (5) can be extended to frequencies that are away from the single particle resonance. This is accomplished through renormalization of the system by dividing it on segments with size $l_r = a(|\varepsilon_m|/\varepsilon_d)^{\nu/(t+s)}$, where t, s and ν are the critical exponents for the static conductivity, dielectric constant, and percolation correlation length, respectively. At the new length scale, the effective dielectric constants of the segments $\varepsilon_m(l_r)$ and $\varepsilon_d(l_r)$ possess the same resonance properties $\varepsilon_m(l_r)/\varepsilon_d(l_r) \simeq -1 + i\kappa$ as the SPs eigenproblem described in the preceding paragraphs. Taking into consideration that the electric field is renormalized as $E_m \sim (l_r/a)E_m^*$ and the new field separation length is $\xi_e \sim (l_r/a)\xi_e^*$, the field moments are estimated as

$$|M_{n,m}| \simeq \left(\frac{|\varepsilon_m'|}{\varepsilon_m''}\right)^{\varkappa_{n,m}} \left(\frac{|\varepsilon_m|}{\varepsilon_d}\right)^{[(n+m-2)\nu+s]/(s+t)} \tag{6}$$

where we have used the scaling relationship $n(l_r) \propto (l_r/a)^{s/\nu}$ for the number of field peaks in each segment. For noble metals we can apply the Drude model for the dielectric constant $\varepsilon_m(\omega) \simeq \varepsilon_b[1 - (\widetilde{\omega}_p/\omega)^2/(1 + i\omega_\tau/\omega)]$, where ε_b is the inter-band transition term, $\widetilde{\omega}_p = \omega_p/\sqrt{\varepsilon_b}$ is the renormalized plasmon frequency, and $\omega_\tau \ll \omega_p$ is the relaxation rate.

In the high frequency range $\omega_p > \omega > \omega_\tau$, we substitute ε_m in Eq. (3) and perform some simple algebraic operations to obtain

$$|M_{n,m}| \simeq (\omega/\omega_\tau)^{\varkappa_{n,m}} \left[\frac{\varepsilon_b}{\varepsilon_d}\left|1-(\widetilde{\omega}_p/\omega)^2\right|\right]^{(n+m-1)/2} \tag{7}$$

where we have also taken into account that in the $2D$ case the critical exponents are roughly equal $t \simeq s \simeq \nu \simeq 4/3$ [12].

Using the exact block elimination method [17] we check Eq. (6) for Ag random films at the percolation threshold. The local field moments $M_{n,0}$ are calculated for large systems ($L = 250$) and are shown in Fig.5. Clearly, there is an excellent correlation between the numerical simulations and the theoretical prediction. In both cases the local fields dramatically increase for incident frequencies that are lower than the renormalized plasmon frequency $\omega < \widetilde{\omega}_p$. Similar correlations between theory and calculations were also observed for the moments $M_{0,m}$.

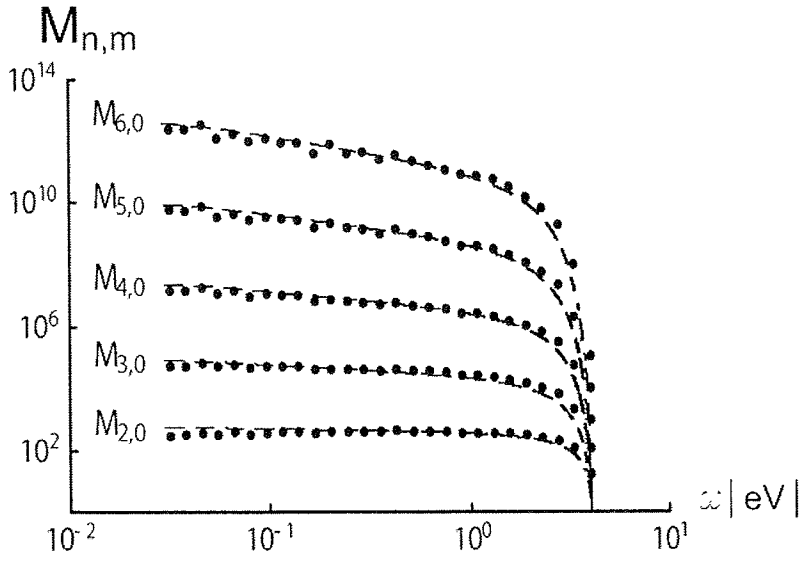

Figure 5: The frequency dependence of the local electric field moments $M_{n,0}$ (dots) calculated with the exact block-elimination method. The numerical results are averaged over 20 different realizations of random metal-dielectric system with size $L = 250$. The analytical curves calculated for exponent $\gamma = 0.14$ (dashed lines) are also included in the graph.

Finally, it is important to note that there is a straightforward relationship between the local field moments $M_{n,m}$ and the strength of various linear and non-linear optical processes occurring at the film surface. For example, the Raman scattering has been found to be strongly enhanced when molecules are deposited on a rough metal-dielectric films [18, 19]. The enhancement factor for this process G_R has been shown to be proportional to the fourth moment of the local fields $M_{4,0}$ [20]. Similarly the enhancement of the Kerr optical

nonlinearity G_K is proportional to the moment $M_{2,2}$ and thus is phase dependent. In the near-infrared spectral range $\omega_p \gg \omega \gg \omega_\tau$ the enhancement factor for those two processes may be estimated as

$$G_R \simeq |G_K| \simeq \varepsilon_d^{-3/2} (\omega_p/\omega_\tau)^3 (\omega_\tau/\omega)^{5\gamma}. \tag{8}$$

where, after substituting the experimentally measured values for the dielectric constant of silver ($\varepsilon_b = 5.0$, $\omega_p = 9.1$ eV and $\omega_\tau = 0.021$ eV [21]), we obtain $G_R \simeq 5 \times 10^6 \varepsilon_d^{-3/2} \omega^{-0.7}$. This result corresponds well with the experimentally measured values of $G_R > 10^6$ [19, 18]. While the maximum enhancement of the Raman scattering from semicontiuous films is lower than what is expected from tuned periodic systems ($G_R \simeq 10^8$[15]), the frequency response here is much broader. Such broad resonance behavior is due to the wide range of cluster sizes present in the percolation films for critical metal concentrations. Also, the increase of the enhancement factor G_R for lower frequencies is a direct manifestation of the underlying SPs localization-delocalization transition. In the case of the classical Anderson localization ($\gamma = 0$), wavelength dependence of the enhancement is not expected. Thus, measurement of the spectral dependence of the efficiencies for wide variety of linear and nonlinear processes may be used for direct measurement of the coupling between the incident electromagnetic waves and the collective (plasmon) electronic response of the random metal-dilectric films.

5 Conclusions

In conclusion, we have investigated the surface plasmons excitation in random metal-dielectric films. The Kirchhoff Hamiltonian that describes this system possess unique short-range correlations between the it diagonal and off-diagonal elements. These correlations, which occur because of the local current conservation, result in a singularity in the density of states and in the localization length of the surface plasmons eigenmodes. Such peculiarities are not present in the non-correlated discrete Anderson analogue. Based on the surface plasmons eigenproblem, we have derived a simple relationship for the local field moments as a function of the incident light frequency and the bulk characteristics of the metal film. The analytical theory is shown to correlate well with the numerical calculations. We also propose experimental studies of linear and non-linear optical processes and their spectral dependencies as a useful tool for direct observation of the surface plasmons localization-delocalization transition in random metal-dielectric composites.

This work was supported in part by NSF grants ECS-0210445 and HRD-0317722 and by NASA grant NCC-1035.

References

[1] P.W. Anderson, *Phys. Rev.* **109**, 1492 (1958).

[2] E. Abrahams, P.W. Anderson, D. C. Licciardello and T. V. Ramakrishnan, *Phys. Rev. Lett.* **42**, 673 (1979).

[3] Il'ya M. Lifshits, Sergei A. Gredeskul and Leonid A. Pastur, *Introduction to the theory of disordered systems*, John Wiley&Sons, Inc (1988).

[4] B. Kramer and A. MacKinnon, *Localization: theory and experiment*, *Rep. Prog. Phys.* **56**, 1469 (1993).

[5] C.M. Soukoulis, E.N. Economou, and G. S. Grest, *Phys. Rev. B* **36**, 8649 (1987).

[6] E. Hofstetter and M. Schreiber, *Phys. Rev. B* **48**, 16979 (1993).

[7] J. C. Flores, *J. Phys.: Condens. Matter* **1**, 8471 (1989).

[8] A. Boliver, *J. Phys. A: Math. Gen.* **25**, 1021 (1992).

[9] M. Hilke, *J. Phys. A: Math. Gen.* **27**, 4773 (1994).

[10] F. A. B. F. de Moura and M. L. Lyra, *Phys. Rev. Lett.* **81**, 3735 (1998).

[11] P. Carpena, P. Bernaola-Galvan, P.Ch. Ivanov and H. E. Stanley, *Nature* **418**, 955 (2002).

[12] D.J. Bergman and D. Stroud, *Solid State Physics* **46**, 147 (1992)..

[13] A.K. Sarychev and V.M. Shalaev, *Physics Reports* **335**, 275 (2000).

[14] S. Gresillon, L. Aigouy, A. C. Boccara, J. C. Rivoal, X. Quelin, C. Desmarest, P. Gadenne, V.A. Shubin, A.K. Sarychev, and V.M. Shalaev, *Phys. Rev. Let.* **82**, 4520 (1999).

[15] D. A. Genov, A. Wei, A. K. Sarychev and V. M. Shalaev, *Nano Lett.* **4**, 153, (2004).

[16] M.I. Stockman, S.V. Faleev, and D.J. Bergman, *Phys. Rev. Lett.* **87**, 167401 (2001).

[17] D. A. Genov, A.K. Sarychev, and V.M. Shalaev, *Phys. Rev. E* **67**, 56611 (2003).

[18] M. Moskovits, *Rev. Mod. Phys.* **57**, 783 (1985).

[19] K. Kneipp, Y. Wang, H. Kneipp, L.T. Perelman, I. Itzkan, R. R. Dasari, and M. S. Feld, *Phys. Rev. Lett.* **78**, 1667 (1997).

[20] A.K. Sarychev and V.M. Shalaev, *Phys. Rev. B* **57**, 13265 (1998).

[21] E.D. Palik (Ed.), *Handbook of Optical Constants of Solids*, (Academic Press, New York, 1985).